Approaches to Solar Cell Design for Pulsed Laser Power Receivers

Geoffrey A. Landis* and Raj K. Jain†

NASA Lewis Research Center
Photovoltaics Branch, 302-1
21000 Brookpark Rd.,
Cleveland, OH 44135

Abstract

Using a laser to beam power from Earth to a photovoltaic receiver in space could be a technology with applications to many space missions. Extremely high average-power lasers would be required in a wavelength range of 700-1000 nm. However, high-power lasers inherently operate in a pulsed format. Existing solar cells are not well designed to respond to pulsed incident power.

To better understand cell response to pulsed illumination at high intensity, the PC-1D finite-element computer model was used to analyze the response of solar cells to continuous and pulsed laser illumination. Over 50% efficiency was calculated for both InP and GaAs cells under steady-state illumination near the optimum wavelength. The time-dependent response of a high-efficiency GaAs concentrator cell to a laser pulse was modeled, and the effect of laser intensity, wavelength, and bias point was studied.

Three main effects decrease the efficiency of a solar cell under pulsed laser illumination: series resistance, L-C "ringing" with the output circuit, and current limiting due to the output inductance.

The problems can be solved either by changing the pulse shape or designing a solar cell to accept the pulsed input. Cell design possibilities discussed are a high-efficiency, light-trapping silicon cell, and a monolithic, low-inductance GaAs cell.

1. Introduction

Laser beaming of power from Earth to space using a photovoltaic array as a laser power converter could be an extremely useful technology, with applications to space missions from low Earth orbit to a lunar base [1-3]. Extremely high average-power lasers would be required, with laser power ranging from hundreds of kilowatts to several megawatts, in a wavelength range of ~700-1000 nm. The high-power laser proposed for this purpose by the NASA SELENE project is the induction free-electron laser (FEL), with a proposed operating wavelength of 840 nm.

Free electron lasers inherently operate in a pulsed format. The output of the proposed induction FEL, for example, consists of a continuous string of pulses approximately fifty nanoseconds wide with 50 µS between pulses, resulting in a duty factor of approximately 1:1000. Other high-power lasers currently available, such as copper-vapor lasers and frequency-doubled Nd:YAG lasers, have similarly pulsed output.

Another type of FEL, the Radio Frequency (RF) FEL, has typically 10-20 pS pulse width and 30-50 nS spacing between pulses. This pulse format is significantly different from the induction laser, and will not be discussed in detail.

Existing solar cells are not well designed to respond to pulsed incident power. An overview of issues involved in using photovoltaic cells for laser conversion can be found in references [4, 5].

In an experiment to test the response of solar cells to the induction free-electron laser pulse, a copper-vapor laser pulse was used. For this experiment the pulse width was 38 nS, with 115 μS spacing between pulses. The wavelength used was 511 nm. The details of this experiment are discussed elsewhere [6,7] and will not be repeated here.

2. Modeling Response of Cells

The PC-1D finite-element computer model was used to model the output of solar cells under laser illumination. Over 50% efficiency was calculated for both InP and GaAs cells under steady-state illumination near the optimum wavelength [8]. For GaAs, this compares well to results measured under laser illumination.

In order to understand the response of a cell to pulsed illumination at high intensity, a high-efficiency GaAs concentrator cell similar to the ones tested in the copper-vapor experiment was modeled. This cell is shown in figure 1. Use of a computer model allows us to observe the output of the cell separated from the circuit interactions which dominate the experimental output; the cell output can then be used as input to the circuit model to understand the array interaction with pulsed incident light.

The response to a single monochromatic light pulse was calculated at 1 nS time intervals. Figure 2 shows the pulse format of the experiment compared to the modeled pulse. A rectangular (step function) illumination pulse was chosen for the model, compared to the slightly rounded pulse of the actual laser. From the response to a rectangular pulse, the response to an arbitrary pulse shape can be found. Some difficulty was found in reaching convergence of the PC-1D algorithm at the abrupt change in current; this problem could usually be resolved by restarting the simulation without reinitializing the conditions.

Figure 3 shows the current output of the cell biased at zero voltage (short circuit), during and after the pulse. The wavelength is 840 nm. The result is shown for four values of peak intensity. At these levels the output does not significantly depend on intensity. Two regimes are visible in the decay of the current after the pulse. There is an initial drop in current which is abrupt on the 1 nS time scale, immediately at the end of the light pulse. This drop comes from current generated in the emitter and space charge region of the cell. Following the immediate drop is a slow decay, with a time constant equal to half the minority carrier lifetime. This decay is quite exponential, as is shown by the straightness of the plot on the semi-log scale.

Since intensity was not seen to be a significant factor in the shape of the decay, a peak intensity of 50 W/cm^2 was used for further simulations.

Figure 4 shows the effect of the incident wavelength. 840 nm is near the GaAs efficiency peak; 511 nm is the wavelength of a copper-vapor laser, and 870 nm is close to the band edge of GaAs. The amount of decrease in current at the end of the pulse depends significantly on the absorption depth of the light, and hence, on the wavelength. Table 1 shows the absorption depths assumed.

The slope of the decay after the initial drop depends only on the minority carrier lifetime and is independent of the wavelength. The slope of this decay is also almost independent of the bias voltage, as shown in figure 5. Here the current axis shows the change in current from the steady-state (dark) conditions. At the peak intensity, the maximum power bias point is about 1 V. Decay at maximum power is almost identical to the short-circuit current decay.

Table 1: Absorption Depth in GaAs

Wavelength λ (nm)	Absorption Depth α^{-1} (μ)
511	0.103
840	0.968
870	1.96
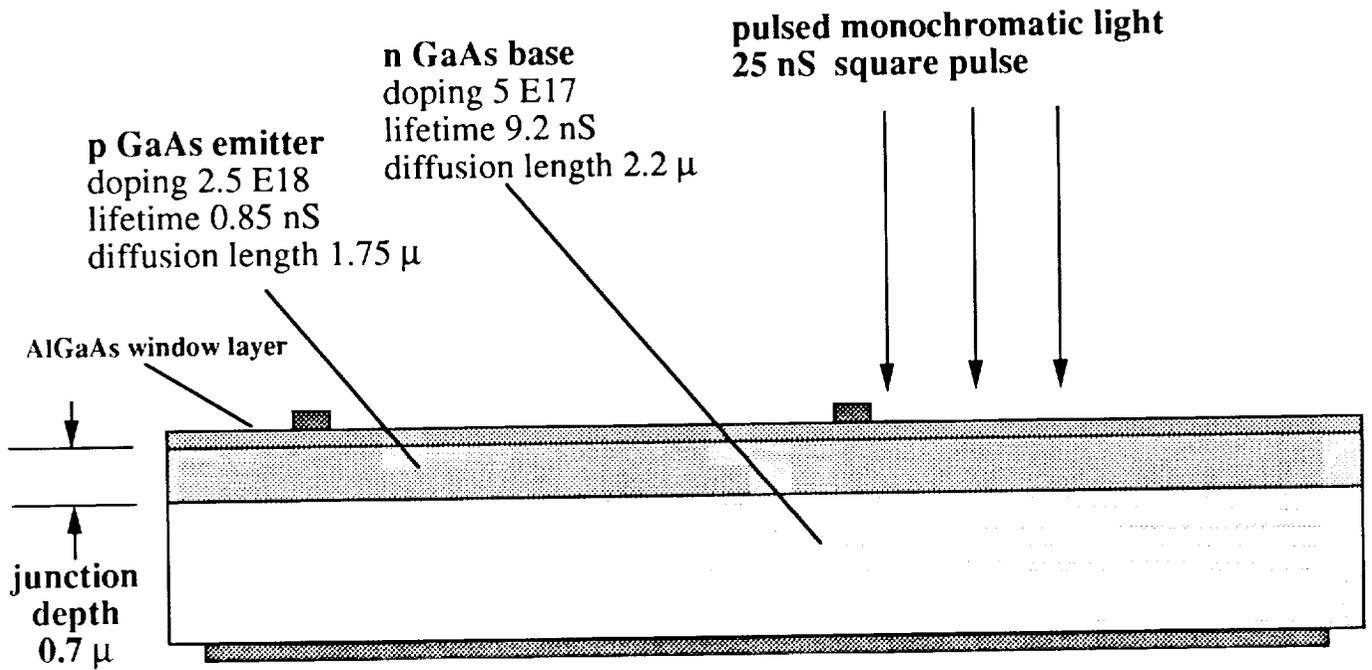
Figure 1. GaAs solar cell model used for computer simulations.
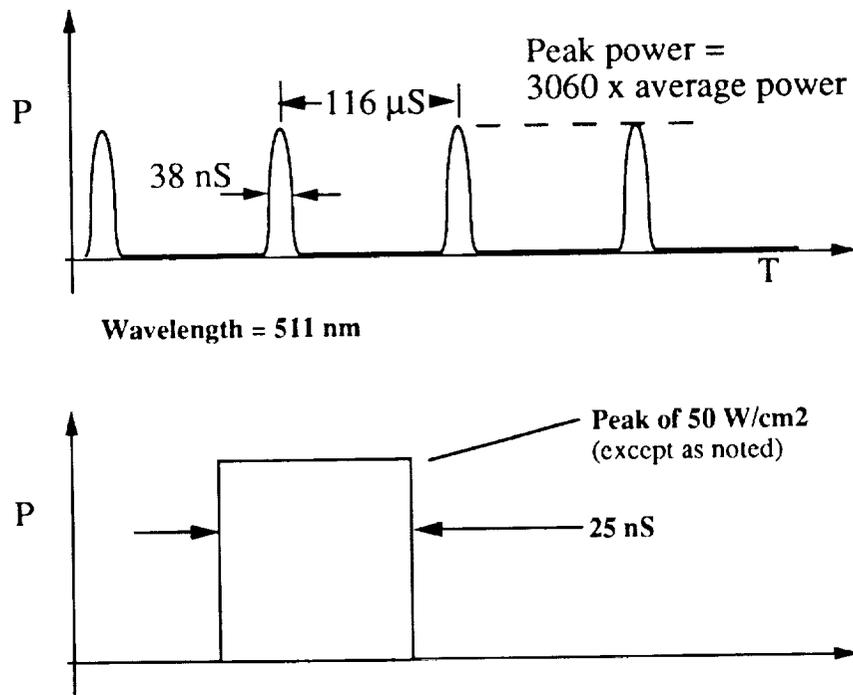
Figure 2. Pulse format of copper-vapor laser (top) and pulse used in computer model (bottom)
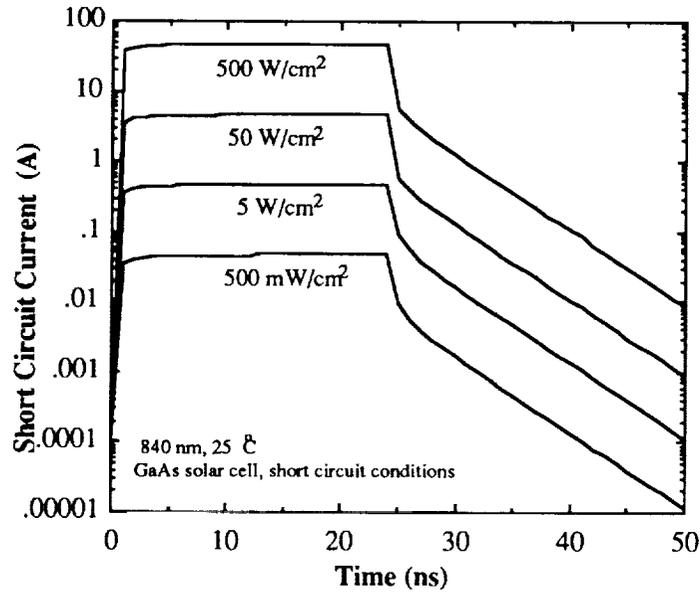
Figure 3. Short circuit current of GaAs cell during laser pulse (semi-log scale) as a function of time, with peak intensity as parameter.
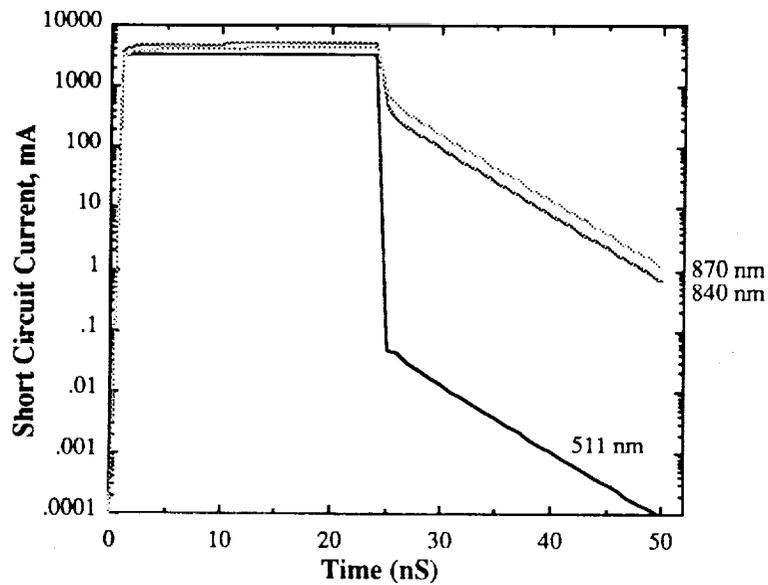
Figure 4. Short circuit current of cell during laser pulse with incident wavelength as parameter. Peak intensity 50 W/cm2.
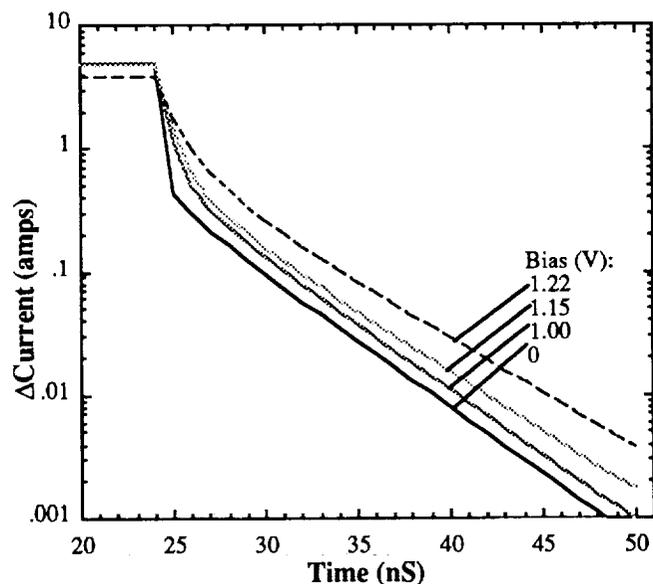
Figure 5. Current output of GaAs cell during laser pulse with cell bias as parameter. Incident pulse 50 W/cm2, 840 nm.
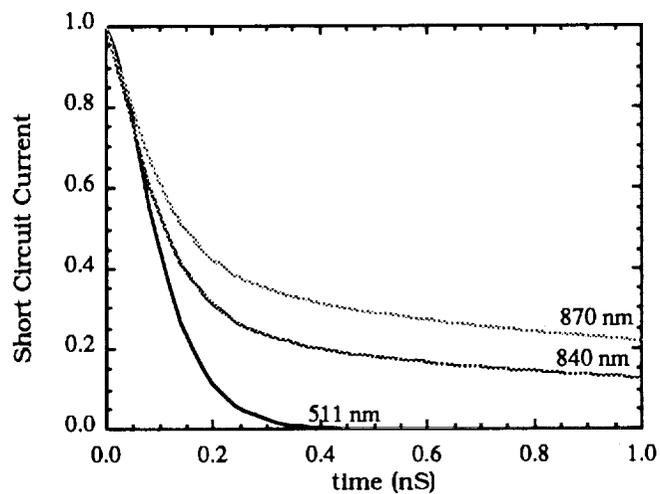
Figure 6. Normalized short circuit current decay in first nanosecond after pulse (linear scale), for 511 nm, 840 nm and 870 nm light pulse.

To examine the initial fast drop in current in more detail, a step-function decrease from steady-state illumination of 50 W/cm^2 to zero was examined in 20 pS time steps. Figure 6 shows this decay for the GaAs cell biased at short circuit. Figure 7 shows the effect of bias voltage. Since the time constant of this decay does not dependent significantly on the minority carrier lifetime, but varies on the minority carrier mobility, this decay is apparently driven by the transit time rather than recombination.

At time scales of many nS characteristic of the induction laser and the copper-vapor laser pulse, it is reasonable to approximate these results for the circuit simulations [7] as showing that the GaAs cell response follows the laser pulse shape. For the copper vapor laser at 511 nm, the pulse broadening is less than 1 nS, which is insignificant considering that the copper-vapor laser pulse itself has a nearly Gaussian decay with constant considerably greater than 1 nS.

3. Circuit Effects on Pulse Illuminated Solar Cells

Three main effects decrease the efficiency of the solar cell in the tests using the pulsed copper-vapor laser:

1. Series Resistance

For the laser format used in the experimental test, the peak power during the pulse (8.6 kHz, 36 nS effective pulse width) is 3200 times the average power. Thus, for short lifetime cells, the peak output current must be 3200 times the average current for the cell to respond. I^2R losses due to the series resistance of the cell reduces the performance severely. For example, the lowest resistance cell measured had a series resistance designed for operation at 800 times solar concentration, well below the 3200x in the experiment.

In addition, the series resistance limits the peak current to:

$$I < V_{oc}/R \qquad (1)$$

For the 0.5 cm diameter GaAs concentrator cells tested, the measured series resistance was about 100 mΩ. At this resistance, series resistance limits the peak current output at a peak intensity of 75 W/cm^2, corresponding to an average power of 75 mW/cm^2 at a peak/average ratio of 1000. At this intensity the current does not significantly increase with further increases in intensity.

2. L-C "Ringing"

Any p-n junction (i.e., solar cell) has a junction capacitance. This, in conjunction with the necessary inductance of the output wiring, results in LC oscillations in the output. Oscillations result in the cell being operated at a bias point away from the peak power point.

3. Output inductance.

The inductance L of the output wiring results in a maximum rate of increase in current:

$$dI/dt \leq V_{oc}/L \qquad (2)$$

and hence, the cell is held at open-circuit voltage for a time

$$t \approx (L\, I_{sc})/V_{oc} \qquad (3)$$

during which it produces little power.

Note that the experiment used wire lengths on the order of 3 cm, far shorter (and hence, far lower inductance) than would be found in an actual flight solar array.

4. Approaches to Solution

The possible solutions to the problem are to either change the light source, or to redesign the photovoltaic receivers:

LASER SOLUTIONS

1. Change the laser to one with a more favorable pulse format
2. Stretch the length of the light pulse
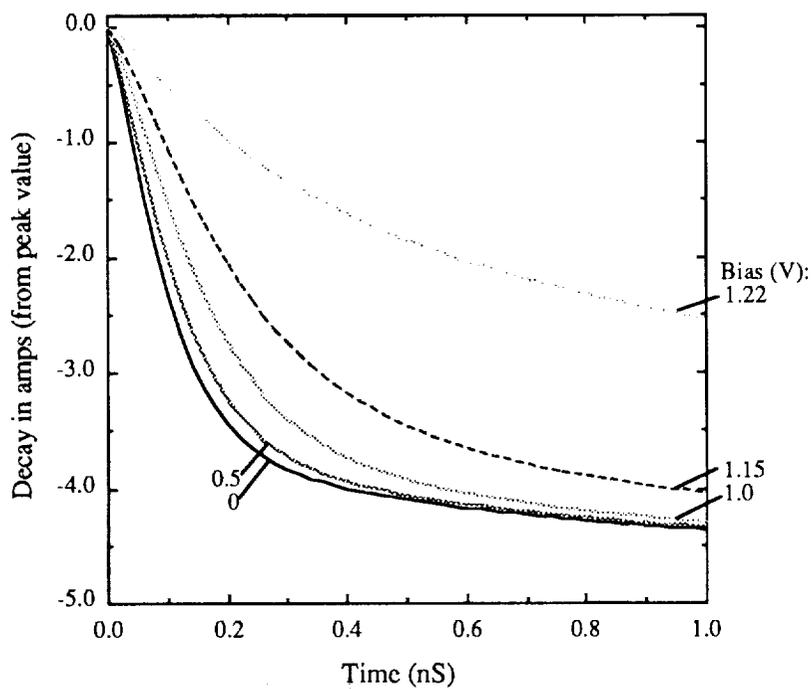
Figure 7. Current decay in first nanosecond of pulse as a function of bias (linear scale; current measured a decrease from illuminated value. Wavelength 840 nm; intensity 50 W/cm2.

3. Redesign existing array and cells to maximize performance with existing output pulse, including reduction of induction and ringing effects and minimization of losses due to series resistance.

4. Design a new cell type to stretch the output and hence, by averaging the output current over a longer period, reduce the peak current value. Three approaches are possible:

a. Improve the minority carrier lifetime on GaAs cell

While low doping, low defects, photon recycling could improve lifetime, it is unlikely that lifetimes could be improved into the microsecond and longer time scales required to average the induction laser pulses. It will also be necessary to reduce the fast portion of the decay curve.

b. Switch to Si cell

Si has an inherently longer lifetime due to the indirect bandgap. The long lifetime means cell output will stretch pulse, making induction effects and series resistance less important.

c. Other techniques to stretch pulse.

Possible methods to stretch the pulse are to use an intermediate phosphor with a long luminescence lifetime, or to collect the radiation to heat an absorber and use thermophotovoltaic cells for conversion.

In this paper, changes to the light source will not be considered. Two approaches will be considered in depth: designing a silicon cell for high response to the laser, and redesigning a GaAs cell for high pulse response.

4.1. High-Efficiency Silicon Solar Cell For Laser Conversion

Silicon is an under-appreciated material for space applications. Existing silicon cells used in space use reliable, but old (circa 1978) technology. The efficiency of currently used silicon cells (for example, SSF cells) is about 13%. However, as shown in table 2, over 20% efficiency has been achieved in several different laboratories across the world.

Table 2: Advanced Silicon Cell Efficiencies Achieved

Solar Efficiency (AM1.5 measurements)

21.3%, (12 cm^2 cell)
University of New South Wales laser-grooved PERL cell [10]
22.3%
Stanford Point Contact Cell (SunPower Corporation) [11]
23.0%
University of New South Wales PERL Cell [12].

Laser Efficiency
(4cm^2 cell)

0.80 μm	34.9%
1.02 μm	45.1%
1.06 μm	39.4%

University of New South Wales PERL Cell. [9].

Silicon, with an indirect bandgap, has minority carrier lifetime on the order of a thousand times longer than that of GaAs. Lifetimes as high as many milliseconds have been achieved. The long minority carrier lifetime of silicon means that the pulse may be stretched, reducing the peak current to a value where series resistance is much less important. Development of a high-efficiency Si cell for laser power beaming will have many potential advantages:

Efficiency potentially comparable to GaAs
Light weight (half the density of GaAs)
Peak monochromatic efficiency at 1.06μ
Expected to have good radiation tolerance (if thin)
Long minority carrier lifetime will average pulsed input into CW output
High efficiency Si cell will have other applications:
    As high-efficiency solar cell for ultra-lightweight space solar arrays
    As low bandgap element of a high-efficiency tandem cell

Existing high-efficiency silicon cells have been measured with over 45% laser efficiency [9]. The requirements, then, are to improve the efficiency another 5% to meet the efficiency goals of the project, and to maintain high performance under expected space radiation conditions.

Silicon is an indirect bandgap semiconductor. This results in a high minority carrier lifetime, which is desirable; however, it also means that the optical absorption coefficient is low (α^{-1}~100 microns at 1.06μ). Low optical absorption means that silicon becomes nearly transparent to light near the bandgap, precisely the wavelengths where monochromatic conversion efficiency ought to be highest. The solution is to increase the optical pathlength within the cell to increase the absorption, without increasing the physical thickness, since the diffusion length decreases with radiation damage. Use of a light trapping structure allows the solar cell to be made thin without loss of light-generated current. Thin Si cells are expected to be extremely radiation tolerant [11].

Long-pathlength light trapping technology has been analyzed in depth [13-15], but has not been used for single-crystal silicon cells to date because there is little motivation to make cells for terrestrial applications thin. One such light trapping design, which increases the average pathlength by more than a factor of 50, is shown in figure 8. Manufacturability of such ultra-thin cells has been discussed in [13].

Using light-trapping, the peak response of a silicon solar cell is expected to shift from 900 nm to slightly over 1 μm. This is not a problem; in fact, the baseline laser wavelength of 840 nm represents a compromise between the long wavelengths desired by the laser designers and the wavelength under 850 nm required by the performance of the GaAs cell. As discussed by Parenti and Primmerman [16], the change of wavelength from the initial baseline of 1.06 μm [17] to the requested 840 nm (which was originally done in order to allow GaAs cells to be used) has increased the difficulty and risk of the adaptive optics design, and it is not known if the optical performance required will even be possible at the shorter wavelength. A return to the 1.06 μm baseline would simplify the adaptive optics design considerably.

An analysis of the response of thin light-trapping Si cells to pulsed laser illumination remains to be done. It is reasonable to expect, but has not yet been demonstrated, that the proposed thin, light-trapping Si cell will retain the desirable pulse-response properties.

4.2 Monolithic Voltage-Adding GaAs Cell Design

An alternative approach is to use a gallium arsenide cell, with the cell and circuit designed to accept the fact that the output will include extremely high current spikes. This requires a redesigned cell structure which has low inductance and series resistance, as well as an output circuit with low inductance and a power management circuit which can accept high peak currents.

One way to accomplish the cell portion of such a design is with a monolithic series structure, as shown in schematic in figure 9.

A monolithic series, or voltage-adding, solar cell is one in which each wafer has many individual sub-cells connected electrically in series. This results in a much larger voltage (N times the voltage of a single cell, where N is the number of subcells connected in series), and a correspondingly lower current. Such a cell may be used, for example, where a voltage higher than a single junction voltage is desired on a single small-area substrate. Monolithic series cells are currently used, for example, as power converters for fiber optic laser illumination [18,19]. Monolithic series interconnection is also useful for operation at high intensity [20], since the electrical series resistance losses are reduced substantially.

Since the subcells are physically small, the distance over which current must flow is reduced, and hence the resistance can decrease. The fractional loss due to series resistance is proportional to the area of the subcell, and hence decreases proportional to N (assuming constant metal coverage and thickness).
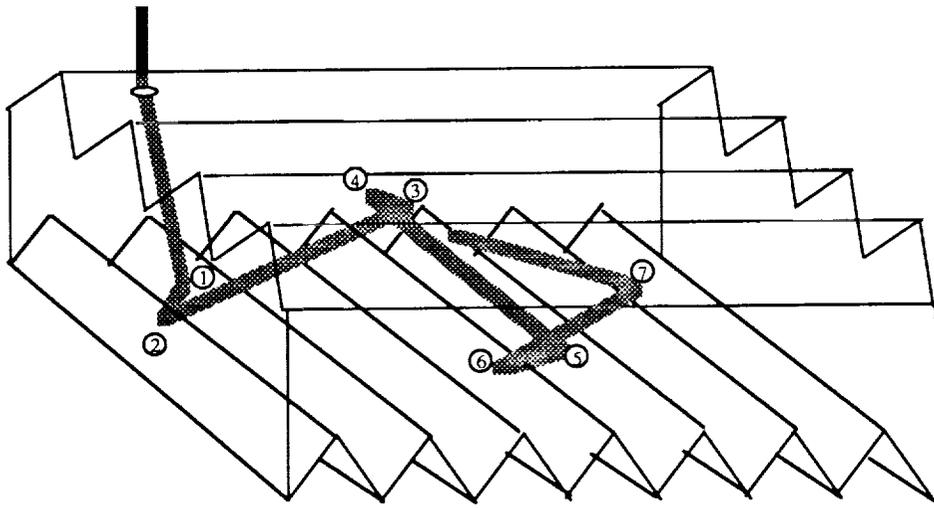
Figure 8. Schematic of cross-grooved light-trapping structure for a thin silicon solar cell, showing typical light path for first two light passages
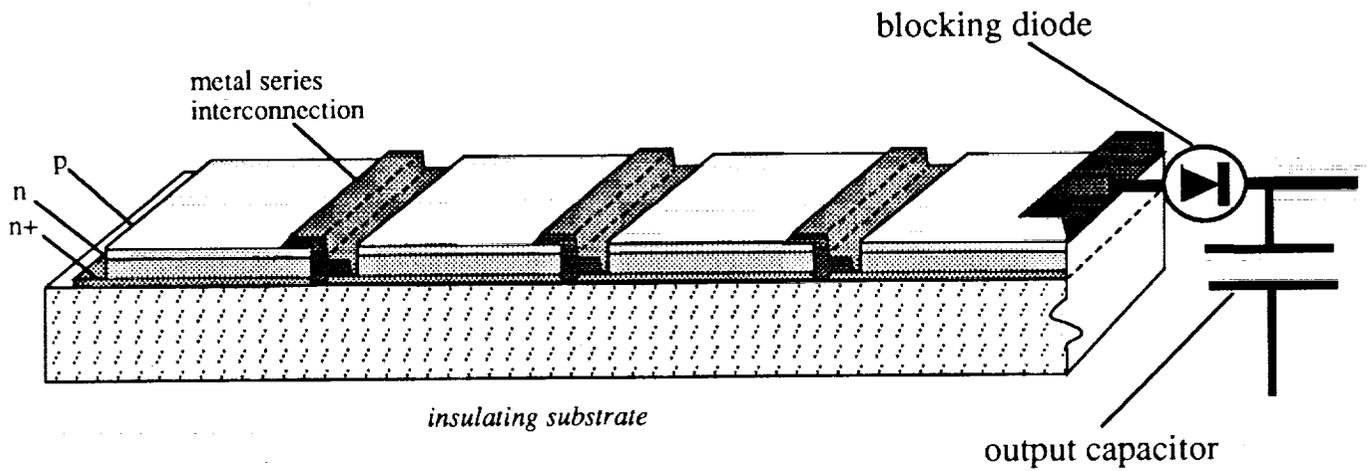
Figure 9. Monolithic voltage-adding GaAs solar cell structure

For pulsed laser illumination, the voltage-adding design has several advantages, as was discussed at the recent workshop on photovoltaics for laser power beaming [21]:

(1) The lower series resistance is an advantage for pulsed laser applications, since the high peak to average intensity ratio results in high peak currents. I^2R losses are especially high if the goal is to operate at the equivalent of many suns of laser intensity, where low series resistance is a major design goal.

(2) Series connected cells allow use of a blocking diode across a high-voltage substring.

An integral diode will reduce dark current. This is important when the duty cycle of the laser is small, since the dark current represents a constant loss when the cell is biased away from zero volts. The diode voltage drop in forward bias is shared among the N subcells, and thus by increasing N the loss due to the blocking diode turn-on voltage drop can be minimized. Such a blocking diode will eliminate the losses associated with the reverse current during the unilluminated portion of the cycle.

Further, by clipping the reverse-current portion of the oscillation, a blocking diode damps the following oscillations.

(3) The series-connected cell has a lower junction capacitance than a single cell of the same area. If N subcell p-n junctions are added electrically in series, the area of each junction is divided by N, and the total capacitance is reduced by a factor of $1/N^2$. This will reduce the LC oscillations.

(4) The series-connected cell allows faster current rise. The current rise in a solar cell with an associated output inductance is limited by the open circuit voltage, $dI/dT \leq L/V_{oc}$ (eq. 2). By connecting N subcells in series, the open circuit voltage is increased by N, and hence the current rise time is faster by a factor of N.

(5) If an output capacitor can be placed at the electrical connections of the cell, or of a group of series interconnected cells, most of the losses due to the electrical pulse interaction with the output wiring can be reduced, since the capacitor will integrate the pulses. By increasing the voltage and decreasing the current compared to a single junction cell, the interconnected cell allows a smaller capacitance and hence lower associated inductance.

Figure 9 shows the important elements of a monolithic voltage-adding design for a GaAs cell, including a blocking diode and integral capacitor. Details common to conventional cell designs, such as an antireflective coating, are not shown. Layer thicknesses are chosen to maximize response at the wavelength of operation. The thickness and doping will also be affected by the need to design for minimum series resistance. A feature not shown is a sawtooth ("prismatic") coverglass to divert light away from the gaps between the cells. Either the p-on-n structure shown, or a n-on-p structure could be used. The distance between subcell elements is set by the maximum allowable resistive loss due to sheet resistance. If larger subcell elements are needed, then a metallization finger pattern running perpendicular to the inter-subcell metallization could be used.

Many monolithic series designs have been proposed [18-26]. The design shown is similar to that of Borden [21].

In addition to cell design, unless all of the current spikes can be integrated by an integral output capacitor, the output wiring must also be designed for low inductance. This requirement leads to short wires, wide and flat conductors, and low magnetic-field design with balanced out and return current paths. A pulse-tolerant power management circuit must also be used, designed using RF design rules. In particular, the shunt regulation circuit must be designed to not dump high transient currents into the shunt.

5. Conclusions

High peak intensities are characteristic of the pulsed output of an induction free-electron laser or a copper-vapor laser. These high intensities presents unique difficulties for photovoltaic receivers, especially for solar cells made from direct-bandgap materials such as GaAs, in which the output of the cell follows the illumination profile on a nanosecond time scale. However, these difficulties do not seem to be insurmountable, and several approaches to design of cells which will accept the high peak intensity pulsed input have been suggested.

165

6. References

1. G.A. Landis, *IEEE Aerospace and Electronic Systems Magazine, Vol. 6,* No. 6, pp. 3-7 (1991); presented at *26th Intersociety Energy Conversion Engineering Conference,* Boston MA, Aug. 1991.

2. C.E. Backus, *Conference Record of the 9th IEEE Photovoltaic Specialists Conference,* Silver Spring MD, pp. 61-65 (1972).

3. G.A. Landis, *Journal of Propulsion and Power, Vol. 8,* No. 1, pp. 251-254 (1992).

4. G.A. Landis, *Photovoltaic Receivers for Laser Beamed Power in Space, NASA Contractor Report 189075* (1991); published in *Conference Record of the 22nd IEEE Photovoltaic Specialists Conference, Vol. 2,* pp. 1494-1502 (1991).

5. L.C. Olsen *et al., Space Photovoltaic Research and Technology 1991, NASA Conference Publication 3121,* pp. 26-1 to 26-9 (1991).

6. B. Anspaugh, R. Mueller, R. Lowe and G. Landis, *Results of Illuminating Various Solar Cells with Pulsed Laser Beams,* NASA Jet Propulsion Laboratory, JPL Publication 92-25, November 1, 1992.

7. R. Lowe, P. Jenkins and G. Landis, *Space Photovoltaic Research and Technology 1992,* NASA Lewis Research Center, Cleveland, OH (1992).

8. R.K. Jain and G.A. Landis, paper 929121, *Proceedings of the 27th Intersociety Energy Conversion Engineering Conference, Vol. 1,* P-259, pp. 1.303-1.307 (1992).

9. J. Zhao, A. Wang, X. Dai, M.A. Green, and S.R. Wenham, *Conference Record of the 22nd IEEE Photovoltaic Specialists Conference, Vol. 1,* pp. 399-402 (1991).

10. R.R. King, R.A. Sinton and R.M. Swanson, *Conference Record of the 20th IEEE Photovoltaic Specialists Conference, Vol. 1,* pp. 538-544 (1988).

11. M.A. Green, *Proceedings of the 10th European Photovoltaics Conference,* pp. 250-253 (1991).

12. M.A. Green, J. Zhao, A. Wang, and S.R. Wenham, *IEEE Electron Device Letters, Vol. 13,* No. 6, pp. 317-318 (1992).

13. G.A. Landis, "A Process Sequence for Manufacture of Ultra-Thin, Light-Trapping Silicon Solar Cells, *Solar Cells, Vol. 29,* pp. 257-266 (1990).

14. P. Campbell and M.A. Green, *Journal of Applied Physics, Vol. 62,* No. 1, pp. 243-249 (1987).

15. G.A. Landis, *Wide Bandgap Heterojunction Window Layers and Optical Confinement for High Efficiency Silicon Solar Cells,* PhD. Thesis, Department of Physics, Brown University (1988).

16. R. Parenti and C. Primmerman, "Power Beaming System Analysis Update," MIT Lincoln Laboratories PBP Memorandum No. 54PM-PBP-001 (15 May 1992).

17. R. Parenti, "Technology Concept Definition for a Ground-Based Power Beaming System," MIT Lincoln Laboratories Report PBP-1 (22 April 1992).

18. M.B. Spitzer *et al.,* "Monolithic Series-Connected GaAs Converter Development," *Conference Record 22nd IEEE Photovoltaic Specialists Conference, Vol. 1,* pp. 142-146 (1991).

19. B. Beaumont *et al.,* "High Efficiency Conversion of Laser Energy and Its Application to Optical Power Transmission," *Conference Record of the 22nd IEEE Photovoltaic Specialists Conference,* pp. 1503-1508 (1991).

20. B. Sater and C. Goradia, "The High Intensity Solar Cell - Key to Low Cost Photovoltaic Power," *Conference Record of the 11th IEEE Photovoltaic Specialists Conference,* pp. 356-363 (1975).

21. SELENE Laser Power Beaming Photovoltaics/FEL Interactions Workshop, NASA Marshall Space Flight Center, Alabama, March 25, 1992.

22. P.G. Borden, *Applied Physics Letters, Vol. 35,* No. 7, pp. 553-554 (1979).

23. B.L. Sater, H.W. Brandhorst, T.J. Riley and R.E. Hart, *Conference Record of the 10th IEEE Photovoltaic Specialists Conference,* pp. 188-193 (1973).

24. A. Gover and P. Stella, *IEEE Transactions Electron Devices, Vol. ED-21,* No. 6, p. 351-356 (1974).

25. R.M. Warner, E.M. Murray, and W.K. Smith, *Applied Physics Letters, Vol. 31,* No. 12, pp. 838-839 (1978).

26. J.C. Evans, A-T. Chai, and C. Goradia, *Conference Record of the 14th IEEE Photovoltaic Specialists Conference,* pp. 194-196 (1980).